TWO-DIMENSIONAL PRESSURE STRUCTURE OF A CORONAL LOOP

V. KRISHAN

Indian Institute of Astrophysics, Bangalore – 560 034, India

(Received 20 August, 1984; in final form 7 February, 1985)

Abstract. The steady-state pressure structure of a solar coronal loop is discussed using the theory of magneto-hydrodynamical turbulence in cylindrical geometry. The steady state is represented by the superposition of two Chandrasekhar–Kendall functions. This representation, in principle can delinetate the three dimensional temperature structure of the coronal loop. In this paper, we have restricted ourselves to a two dimensional modeling since only this structure submits itself to the scrutiny of the available observations. The radial as well as the axial variations of the pressure in a constant density loop are calculated. These variations are found to conform to the observed features of cool core and hot sheath of the loops as well as to the location of the temperature maximum at the apex of the loop. We find that these features are not present uniformly all along either the length of the loop or across the radius as will be shown in the text. We have also discussed the possible oscillatory nature of these pressure variations and the associated time periods have been estimated.

1. Introduction

The loop or the arch like configuration of the solar active regions has been seen in the emission at UV, EUV, and X-ray wavelengths (Foukal, 1978; Levine and Withbroe, 1977; Vaiana and Rosner, 1978). The current carrying plasma in the loop supports a helical form of the magnetic field (Poletto *et al.*, 1975; Krieger *et al.*, 1976; Hood and Priest, 1979). In earlier papers (Krishan, 1983a, b) the steady-state of a coronal loop was derived by using Taylor's hypothesis that the steady-state of a nonlinear turbulent plasma is a state of minimum energy with a constant value of the magnetic helicity and this state is represented by a superposition of force-free states describable by Chandrasekhar–Kendall functions, Taylor (1974), Montgomery *et al.* (1978). The magnetic and the velocity fields are expanded in terms of Chandrasekhar–Kendall functions. Using the MHD equations, the pressure profile is then calculated as a function of the velocity and the magnetic fields. The present work is an extension of the earlier work (Krishan, 1983a, b) on coronal loop modeling where only the radial temperature structure was derived by assuming the plasma to be in a single Chandrasekhar–Kendall function. In this piece of work, we choose to represent the loop plasma through the superposition of two Chandrasekhar–Kendall functions. This brings in the three-dimensional spatial variation (r, θ, z) in the plasma parameters and the state does not correspond to a force-free state. We have confined ourselves to study the two-dimensional (r, z) variations of the plasma temperature as the observational results on the azimuthal variations are not available so far. In the next section, the MHD equations used to derive the temperature profile are presented. The calculated profiles are shown graphically in several diagrams which exhibit the rather non-uniform

Solar Physics **97** (1985) 183–189. 0038–0938/85.15.

behaviour of the plasma temperature. This study provides an alternative way of describing MHD equilibrium in terms of the conserved quantities like the total energy, the magnetic helicity and the magnetic fluxes. One can study the statistical mechanics of the velocity and the magnetic fields (Krishan, 1985). Tsinganos (1981, 1982a, b) has studied the equilibrium of an ideal MHD system by treating magnetic vector potential as a variable. Some of the solutions of the MHD equations do conform to the force free twisted magnetic field geometry used in the present work.

2. Steady-State Model of Coronal Loops

We represent a coronal loop by a cylindrical column of plasma with periodic boundary conditions at the ends of the cylinder ($z = 0, L$). The pressure (p) profile of an incompressible MHD plasma is given by

$$\nabla^2 p = \nabla \cdot [(\nabla \times \mathbf{B}) \times \mathbf{B}] - \nabla \cdot [(\mathbf{V} \cdot \nabla)\mathbf{V}], \qquad (1)$$

where $\mathbf{V}$, $\mathbf{B}$ are respectively the velocity and the magnetic field. The magnetic field $\mathbf{B}$ is defined in Alfvén speed units, i.e. $\mathbf{B} \equiv \mathbf{B}/\sqrt{4\pi\rho}$. Gravity is neglected.

We represent the loop plasma to be in a state produced by the superposition of two Chandrasekahr–Kendall functions corresponding to ($n = m = 0$) and ($n = 1$, $m = 0$) Montgomery *et al.* (1978). The corresponding fields are given as

$$\mathbf{B} = \mathbf{B}_0 + \mathbf{B}_1,$$

where

$$\mathbf{B}_0 = \xi_0 \lambda_0 C_0 [\hat{e}_\theta \lambda_0 J_1(\gamma_0 r) + \hat{e}_z \lambda_0 J_0(\gamma_0 r)] e^{ik_1 z},$$

$$\mathbf{B}_1 = \xi_1 \lambda_1 C_1 \left[-\hat{e}_r \left(\frac{ik_1 \gamma_1}{\lambda_1}\right) J_1(\gamma_1 r) + \hat{e}_\theta \gamma_1 J_1(\gamma_1 r) + \hat{e}_z \left(\frac{\lambda_1^2 - k_1^2}{\lambda_1}\right) J_0(\gamma_1 r)\right] e^{ik_1 z}, \qquad (2)$$

$$\mathbf{V} = \mathbf{V}_0 + \mathbf{V}_1, \qquad \mathbf{V}_0 = \frac{\eta_0}{\xi_0} \mathbf{B}_0,$$

$$\mathbf{V}_1 = \frac{\eta_1}{\xi_1} \mathbf{B}_1, \qquad \xi(0, 0, 1) \equiv \xi_0, \qquad \xi(1, 0, 1) \equiv \xi_1, \quad \text{etc.} \qquad (3)$$

Substituting for $\mathbf{V}_0$, $\mathbf{V}_1$, $\mathbf{B}_0$ and $\mathbf{B}_1$ we get the following set of simultaneous partial differential equations:

$$\frac{\partial p}{\partial r} = (C_0 \lambda_0 \eta_0)^2 \frac{1}{r} \left(\frac{\partial J_0(\gamma_0 r)}{\partial r}\right)^2 - C_0 C_1 \lambda_0 \lambda_1 \eta_0 \eta_1 \, e^{ik_1 z} \times$$

$$\times \frac{\partial}{\partial r}\left[\frac{\partial}{\partial r} J_0(\gamma_0 r) \frac{\partial J_0(\gamma_1 r)}{\partial r} + \frac{\lambda_0}{\lambda_1} \gamma_1^2 J_0(\gamma_0 r) J_0(\gamma_1 r)\right],$$

$$\frac{\partial p}{\partial \theta} = 0,$$

$$\frac{\partial p}{\partial z} = -ik_1 C_0 C_1 \eta_0 \eta_1 \lambda_0 \lambda_1 e^{ik_1 z} \times$$

$$\times \left[\frac{\partial J_0(\gamma_0 r)}{\partial r} \frac{\partial J_0(\gamma_1 r)}{\partial r} + \frac{\lambda_0}{\lambda_1} \gamma_1^2 J_0(\gamma_0 r) J_0(\gamma_1 r) \right] . \tag{4}$$

We have also assumed equipartition of energy between the velocity and the magnetic fields at the scales λ_0 and λ_1. This permits us to put $\eta_0 = \xi_0$ and $\eta_1 = \xi_1$. Integration of Equation (4) yields:

$$\begin{aligned} p = p_0 &+ (C_0 \lambda_0 \eta_0 \gamma_0)^2 \tfrac{1}{2} [1 - J_0^2(\gamma_0 r) - J_1^2(\gamma_0 r)] - \\ &- 2 C_0 C_1 \lambda_0 \lambda_1 \eta_0 \eta_1 [\gamma_0 \gamma_1 J_1(\gamma_0 r) J_1(\gamma_1 r) \cos k_1 z + \\ &+ (\lambda_0/\lambda_1) \gamma_1^2 J_0(\gamma_0 r) J_0(\gamma_1 r) \cos k_1 z - (\lambda_0/\lambda_1) \gamma_1^2], \end{aligned} \tag{5}$$

where $p = p_0$ at ($r = 0$, $z = 0$).

The normalization constants C_0 and C_1 are found to be:

$$\begin{aligned} |C_1|^2 = (2\pi L)^{-1} &\left[\left(\frac{\gamma_1 R}{2} \right)^2 \left(1 + \frac{k_1^2}{\lambda_1^2} \right) \{ J_1^2(\gamma_1 R) - \right. \\ &\left. - J_0(\gamma_1 R) J_2(\gamma_1 R) \} + \frac{(\gamma_1 R)^2}{2} \frac{\gamma_1^2}{\lambda_1^2} \{ J_0^2(\gamma_1 R) + J_1^2(\gamma_1 R) \} \right]^{-1} \end{aligned} \tag{6}$$

and

$$\begin{aligned} |C_0|^2 = (2\pi L)^{-1} &\left[\frac{(\gamma_0 R)^2}{2} \{ 2 J_1^2(\gamma_0 R) - J_0(\gamma_0 R) \times \right. \\ &\left. \times J_2(\gamma_0 R) + J_0^2(\gamma_0 R) \} \right]^{-1} . \end{aligned} \tag{7}$$

λ_1 is given by the zeros of $J_1(\gamma_1 R)$. We find $\gamma_1 R \simeq 3.8$, $\lambda_1 R \simeq 4$. λ_0 is determined from the relationship

$$\frac{\psi_t}{\psi_p} = -\frac{R}{L} \frac{\gamma_{00q} J_0'(\gamma_{00q} R)}{\lambda_{00q} J_0(\gamma_{00q} R)}, \tag{8}$$

where ψ_t and ψ_p are the toroidal and poloidal magnetic fluxes. We shall calculate λ_0 for two values of the ratio ψ_t/ψ_p and calculate $p(r, z)$ for each case.

Case I

Let the ratio of the length to the radius be $L/R = 5$. Assuming $\psi_t/\psi_p = 0.1$ gives a value for $\lambda_0 R = \gamma_0 R = 1$. The relative contribution of the two modes (0, 0, 1) and (1, 0, 1) is fixed by assuming that there is less energy in the smaller spatial scale or for Case I:

$$\eta_0^2\lambda_0^2 > \eta_1^2\lambda_1^2 \quad \text{or} \quad \frac{\eta_1}{\eta_0} < \frac{\lambda_0}{\lambda_1} = 0.25.$$

As an illustration, we choose $\eta_1/\eta_0 = 0.2$. From Equations (6) and (7) we estimate:

$$C_0 = 1.5034\,(2\pi L)^{-1/2}; \qquad C_1 = 0.6505\,(2\pi L)^{-1/2}.$$

The total energy E is given by

$$E = 2(\lambda_0^2\eta_0^2 + \lambda_1^2\eta_1^2).$$

The numerical results are presented for $E/\pi R^2 L = 1$ erg cm^{-3}. Using Equation (5) we plot pressure as a function of r for several values of z in Figure 1a and pressure as a function of z for several radial positions in Figure 1b. Figure 1a shows that the pressure or temperature (for constant density) increases towards the surface of the loop at the bottom ($z = 0$). It is approximately constant across the radius at the mid point of the half-loop ($z = L/4$) and at the apex of the loop ($z = L/2$) the pressure is maximum at

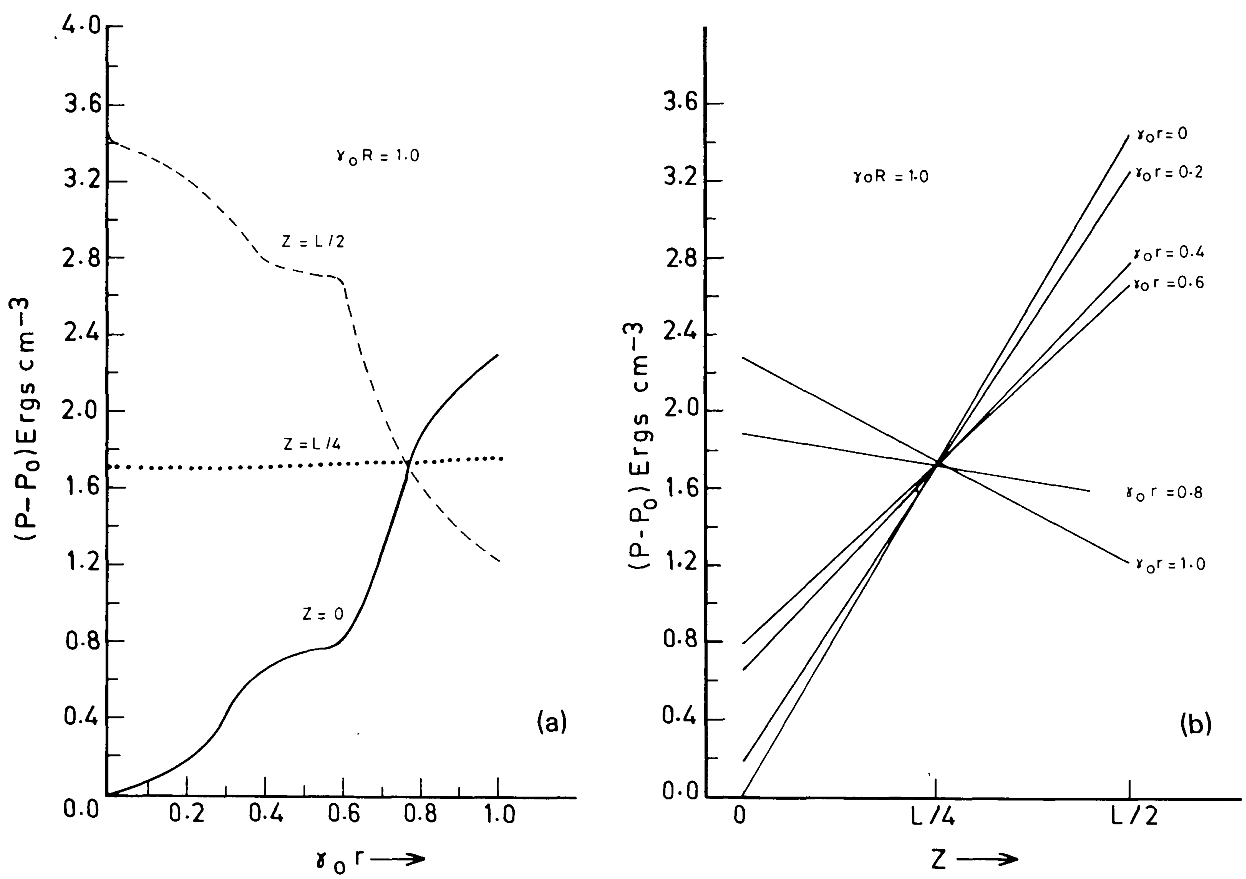

Fig. 1. Pressure variations for Case I. (a) Radial variation. (b) Axial variation for radial positions indicated on the lines.

the axis and decreases towards the surface. Figure 1b shows a linear axial increase in pressure at radial positions near ($r = 0$) and a linear axial decrease of pressure near the surface ($r = R$). The pressure is maximum at ($r = 0$, $z = L/2$). The plasma acquires a twisted configuration. The values of the magnetic helicity H_m and the toroidal flux ψ_t which are the invariants of the system can be estimated from the following defining relationships:

$$H_m = \lambda_0 \,|\xi_0|^2 + \lambda_1 \,|\xi_1|^2 = (\lambda_0 \eta_0^2 + \lambda_1 \eta_1^2),$$

$$\eta_0^2 \lambda_0^2 = E/3.28 \quad \text{for} \quad \eta_1/\eta_0 \simeq 0.2.$$

Assuming $E \simeq 10^{28}$ ergs (Levine and Withbroe, 1977), we find: $H_m = 0.3 \times 10^{37}$ erg cm, and $\psi_t = 2\pi R \xi_0 \gamma_0 C_0 J_1(\gamma_0 R) = 6.7 \times 10^{17}$ maxwells for a loop of volume $= 10^{28}$ cm^3 and length $L = 4.3 \times 10^9$ cm.

Case II

$$\gamma_0 R = 5.4 \quad \text{for} \quad \psi_t/\psi_p = 1.6,$$

$$C_0 = (2\pi L)^{-1/2} \times 0.5334,$$

and here

$$\eta_1^2 \lambda_1^2 > \eta_0^2 \lambda_0^2 \quad \text{or} \quad \frac{\eta_0}{\eta_1} < \frac{\lambda_1}{\lambda_0} = \frac{4}{5.4} = 0.7;$$

choose

$$\eta_0/\eta_1 = 0.4.$$

Figure 2a shows the radial variation of pressure for the three values of z. The behaviour is qualitatively different in this case. The pressure shows radial oscillations at the bottom ($z = 0$) as well as at the top of the loop ($z = L/2$). The oscillations at the two axial positions are out of phase and thus form a stationary wave pattern. The spatial period is approximately $1/\gamma_0 = R/5.4$. If one wants to associate time period to these oscillations, one needs to study the dynamics of this state which is not being done presently. One could make what one may call a learned guess by finding the value of the radial velocity V_r which itself is a function of the space coordinates. The time period $T_r \simeq (R/5.4)/(1/|V_r|)$, where

$$V_r^2 = \eta_1^2 C_1^2 k_1^2 \gamma_1^2 J_1^2(\gamma_1 r).$$

Maximizing $J_1^2(\gamma_1 r) \simeq (0.58)^2$ at $\gamma_1 r = 1.8$ we find $T_r \simeq 2.5$ min. The radial variation at $z = L/4$ corresponds to rise in pressure for small r and saturation near the surface. The axial variation of pressure is shown in Figure 2b. The values of the magnetic helicity and the toroidal flux are respectively 0.1×10^{37} erg cm and (-2×10^{17}) maxwells.

From Equation (5), one notices that the axial variation of pressure is also periodic with a spatial period $1/L$. The corresponding time period could be calculated by knowing the magnitude of the root mean square axial velocity. We find time periods for axial variations of the order of few minutes. Finally, for the sake of comparisons, the radial

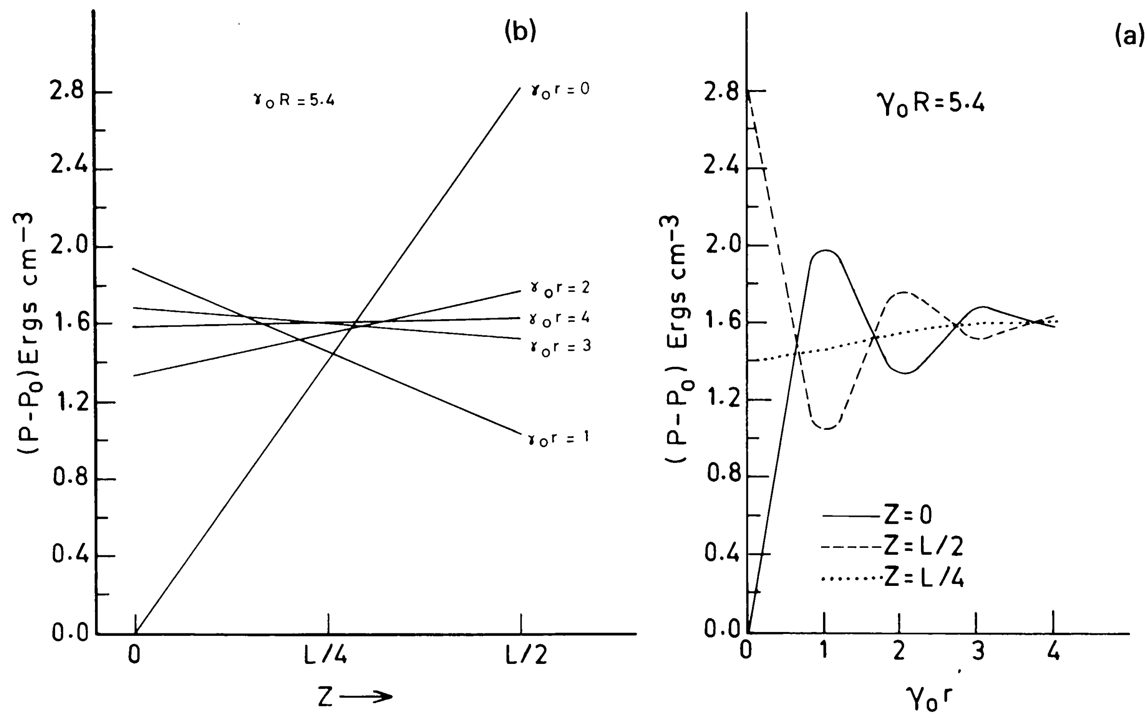

Fig. 2. Same as Figure 1 for Case II.

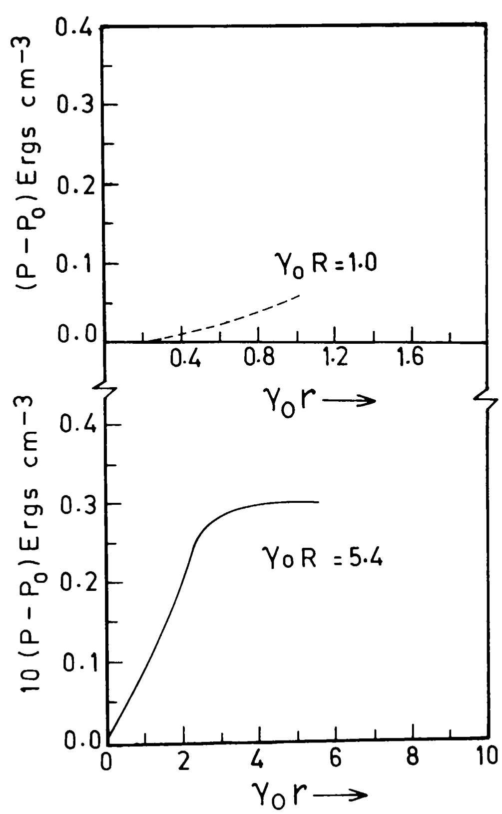

Fig. 3. Radial pressure profile in a force-free configuration.

pressure profile of the loop plasma in a force-free configuration represented by a single Chandrasekhar–Kendall function $n = m = 0$ is shown in Figure 3. This configuration has been discussed in the earlier work (Krishan, 1983b).

3. Conclusions

Representation of the coronal loop plasma in a state generated by the superposition of two Chandrasekhar–Kendall functions leads to a two-dimensional spatial profile of the plasma pressure. It is found that the radial variation of pressure corresponding to the larger spatial widths of the hotter lines does not exist all along the length of the loop. A twisted configuration of the plasma is obtained. The pressure or the temperature is still maximum at the top of the loop but only near the axis. For smaller spatial scales which are determined from the ratio of the toroidal to poloidal magnetic fluxes, the radial pressure variation exhibits oscillations. Estimates of magnetic helicity are given which could be checked whenever such observations become available.

References

Foukal, P. V.: 1978, *Astrophys. J.* **223**, 1046.
Hood, A. W. and Priest, E. R.: 1979, *Astron. Astrophys.* **77**, 233.
Krieger, A. S., de Feiter, L. D., and Vaiana, G. S.: 1976, *Solar Phys.* **47**, 117.
Krishan, V.: 1983a, *A Steady State Model of Active Region Coronal Loops.* Proceedings of College on Radiation in Plasmas, Trieste, 1983.
Krishan, V.: 1983b, *Solar Phys.* **88**, 155.
Krishan, V.: 1985, *Solar Phys.* **95**, 269.
Levine, R. H. and Withbroe, G. L.: 1977, *Solar Phys.* **51**, 83.
Montgomery, D., Turner, L., and Vahala, G.: 1978, *Phys. Fluids* **21**, 757.
Poletto, G., Vaiana, G. S., Zomback, M. V., Krieger, A. S., and Timothy, A. F.: 1975, *Solar Phys.* **44**, 83.
Taylor, J. B.: 1974, *Phys. Rev. Letters* **33**, 1139.
Tsinganos, K. C.: 1981, *Astrophys. J.* **245**, 764.
Tsinganos, K. C.: 1982a, *Astrophys. J.* **252**, 775.
Tsinganos, K. C.: 1982b, *Astrophys. J.* **259**, 820.
Vaiana, G. S. and Rosner, R.: 1978, *Ann. Rev. Astron. Astrophys.* **16**, 393.